Supplementary Materials

Supplemental Acknowledgements

The study groups include: Nipat Teeratakulpisarn[1], Supanit Pattanachaiwit[1], James Fletcher[1], Ponpen Tantivitayakul[1], Duanghathai Suttichom[1], Peeriya Prueksakaew[1], Kultida Poltavee[1], Jintana Intasan[1], Tassanee Luekasemsuk[1], Hathairat Savadsuk[1], Somporn Tipsuk[1], Nisakorn Ratnaratorn[1], Kamonkan Tangnaree[1], Chutharat Munkong[1], Rommanus Thaimanee[1], Patcharin Eamyoung[1], and Sasiwimol Ubolyam[1], Robert O'Connell[2], Alexandra Schuetz[2], Denise Hsu[2], Tanyaporn Wansom[2], Siriwat Akapirat[2], Bessara Nuntapinit[2], Nantana Tantibul[2], Nampueng Churikanont[2], Saowanit Getchalarat[2], Ellen Turk[3,4], Corinne McCullough[3,4], Oratai Butterworth[3,4], Madelaine Ouelette[3,4], Mark Milazzo[3,4], and Leigh Anne Eller[3,4]

[1]SEARCH, The Thai Red Cross AIDS Research Centre, Bangkok 10330, Thailand.

[2] Department of Retrovirology, Armed Forces Research Institute of Medical Sciences United States Component, Bangkok 10400, Thailand.

[3]U.S. Military HIV Research Program, Walter Reed Army Institute of Research, Silver Spring, MD 20910, USA.

[4]Henry M. Jackson Foundation for the Advancement of Military Medicine, Bethesda, MD 20817, USA.

Supplemental Figures

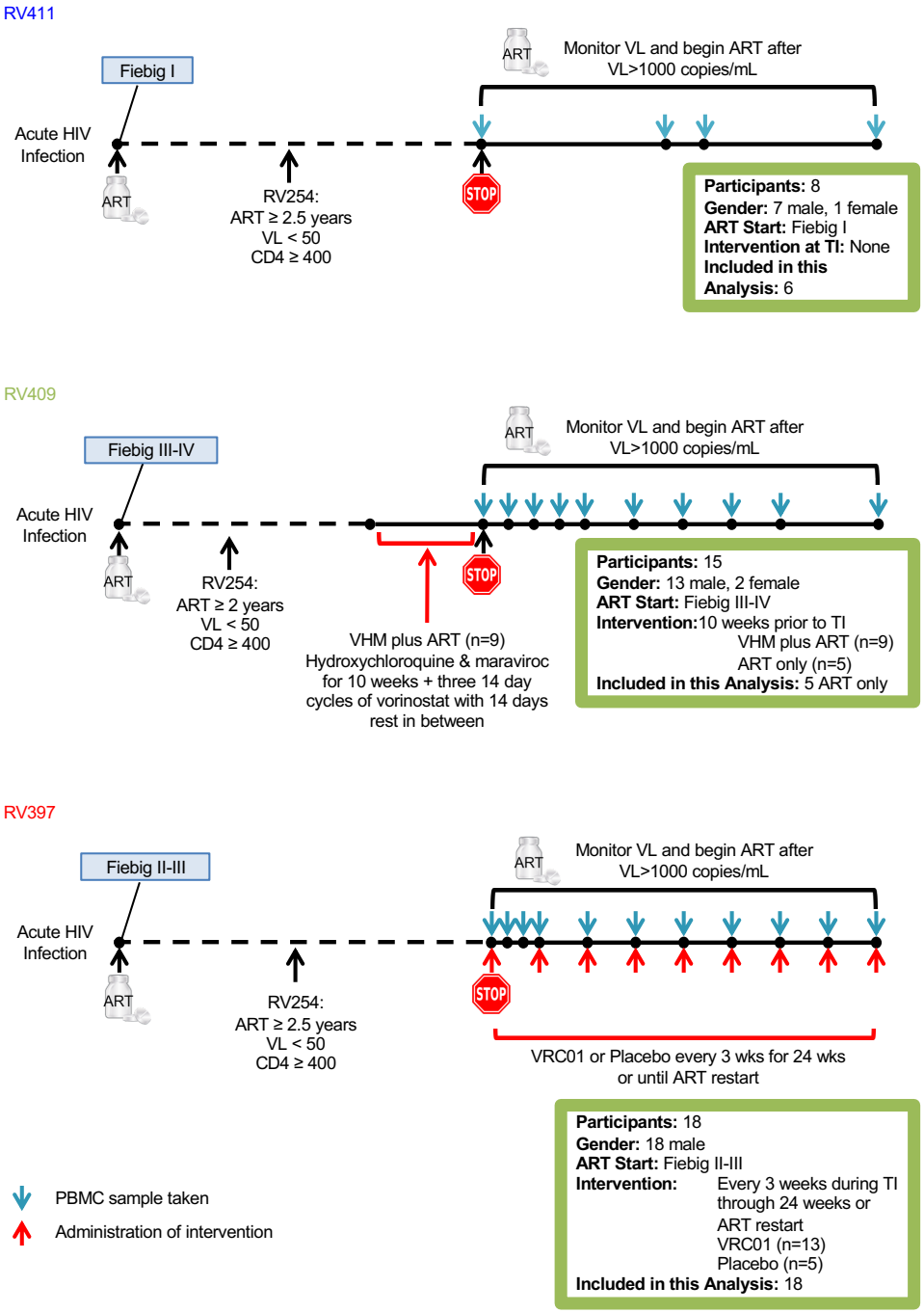

Supplemental Figure 1. ATI study design. Participants were enrolled in one of three ATI studies which occurred in Thailand. RV411 included 8 participants who were treated in Fiebig stage I of AHI and received no intervention at the time of ATI. RV409 included 15 participants who started ART in Fiebig stages III-IV, only 14 of whom interrupted ART. Nine participants in RV409 received vorinostat, hydroxychloroquine, and maraviroc in addition to ART for ten weeks prior to ATI. RV397 included 18 participants who started ART during Fiebig stages II-III of acute infection. Thirteen participants in this study received infusions of the VRC01 antibody at three-week intervals after ATI.

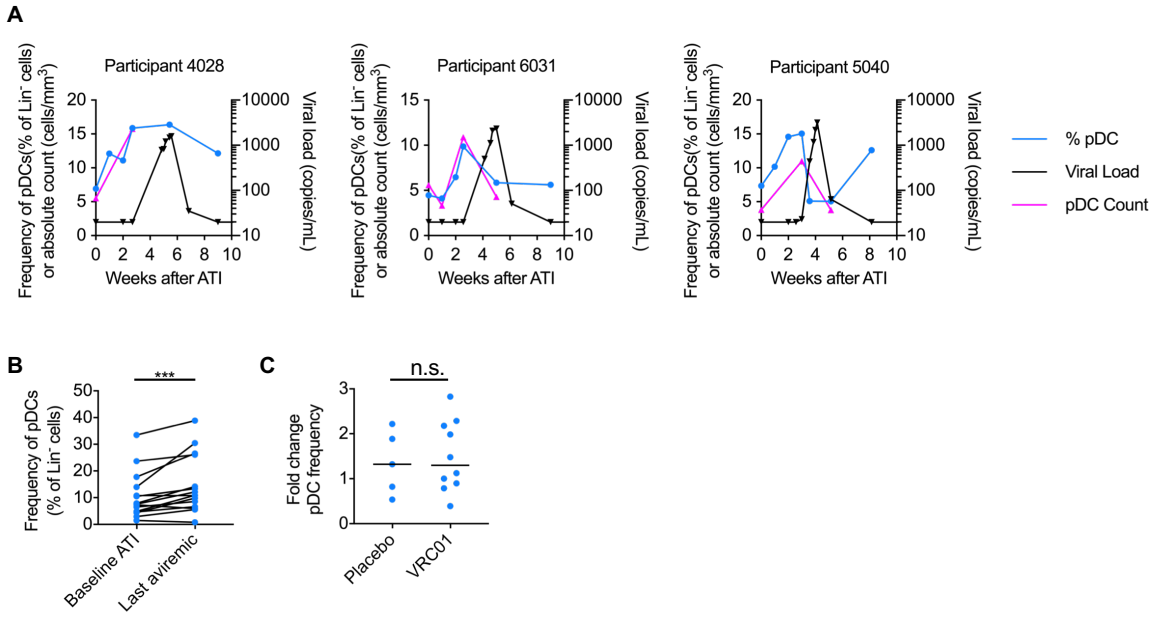

Supplemental Figure 2. Comparison of pDC frequency with pDC absolute count and between treatment arms. *(A)* pDC absolute count was determined in RV397 participants at time points when the absolute $CD4^+$ T cells count was measured at the time of sampling. Absolute pDC count was calculated using the number of pDCs measured by flow cytometry and the ratio of the absolute $CD4^+$ T cell count to the number of $CD4^+$ T cells measured by flow cytometry. Shown are the pDC frequency (blue) and absolute pDC count (pink) for three participants for whom pDC counts could be calculated prior to detection of plasma viremia. *(B)* The frequency of pDCs was compared between the baseline time point at treatment interruption and the last aviremic point after ATI in participants who received no therapeutic intervention. n = 15 (*** *p<0.001*, Wilcoxon test). *(C)* The median fold change in pDC frequency between baseline ATI and the last aviremic time point was compared between participants in the placebo and treatment arms of RV397. Data were analyzed with the Mann-Whitney test. n = 5 placebo, 10 treatment.

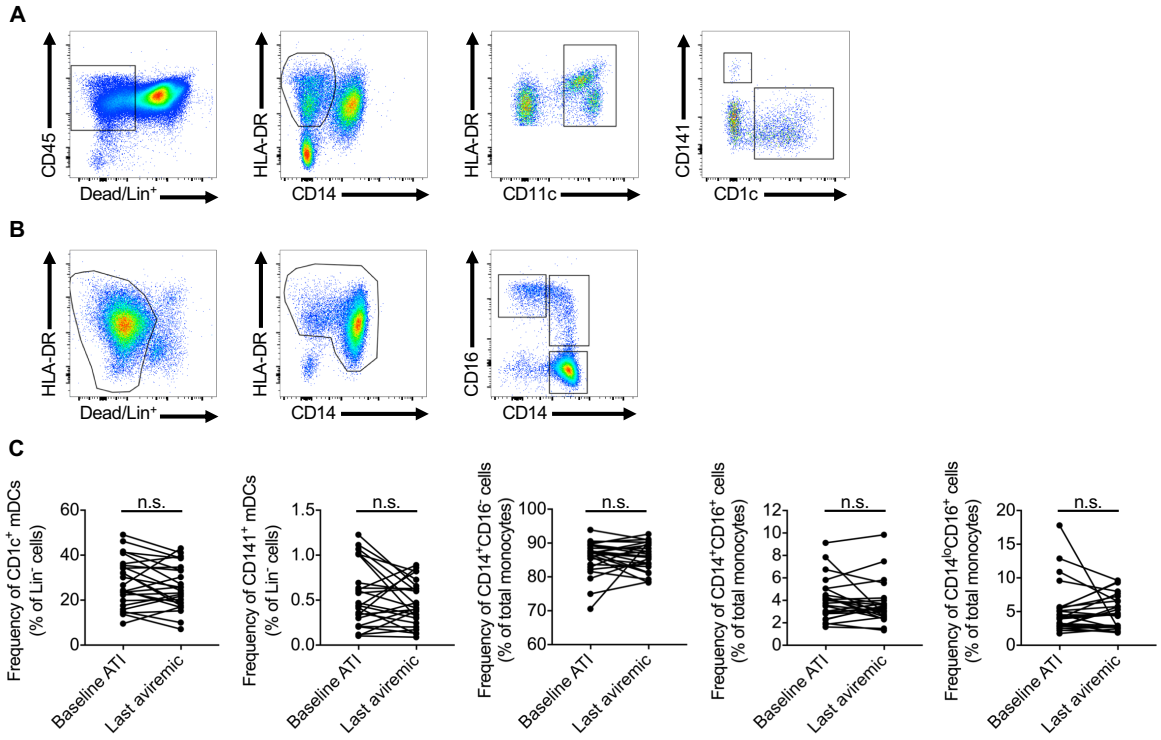

60

61 **Supplemental Figure 3. Changes in mDC and monocyte frequencies after ATI.**

62 *(A)* CD1c$^+$ and CD141$^+$ mDCs in the blood were identified within the CD45$^+$HLA-DR$^+$CD11c$^+$

63 lineage negative cells (CD3$^-$CD14$^-$CD19$^-$CD56$^-$) by flow cytometry. *(B)* Classical

64 (CD14$^+$CD16$^-$), intermediate (CD14$^+$CD16$^+$), and nonclassical (CD14$^-$CD16$^+$) monocytes were

65 identified within the lineage negative (CD3$^-$CD19$^-$CD56$^-$) HLA-DR$^+$ population. *(C)* The

66 frequencies of dendritic cell and monocyte populations at baseline ATI and the last aviremic time

67 point are shown. Dendritic cell frequencies were measured as a percentage of the HLA-DR$^+$

68 lineage negative cells. n = 25, 10 of whom received VRC01.

69

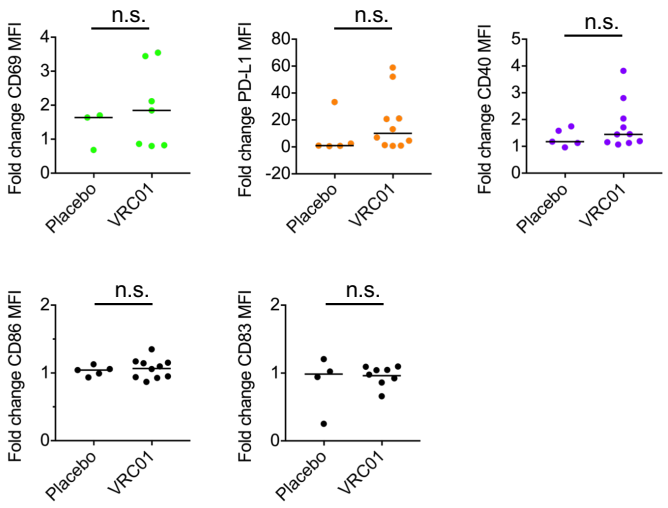

Supplemental Figure 4. Comparison of surface marker expression between arms of RV397. The median fold change in MFI of CD69, PD-L1, CD40, CD86, and CD83 between baseline ATI and the last aviremic time point was compared between participants in the placebo and treatment arms of RV397. Data were analyzed with the Mann-Whitney test. n = 5 placebo, 10 treatment.

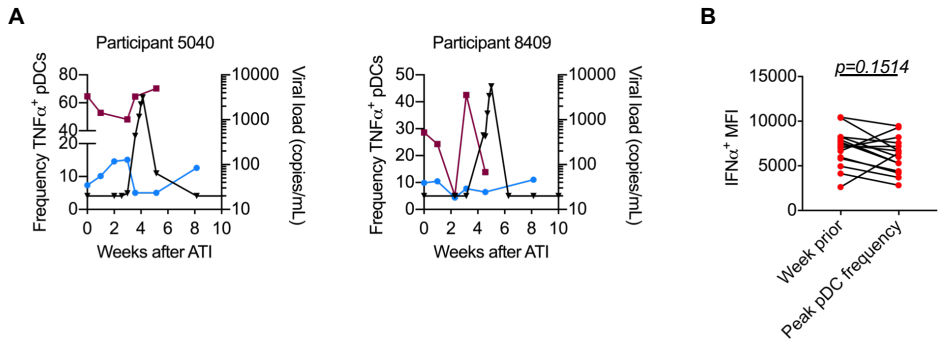

Supplemental Figure 5. Cytokine production by pDCs after in vitro activation.

(A) The percentages of pDCs that produced TNFα in response to imiquimod stimulation (maroon) are shown. pDC frequency (blue) and HIV-1 viral load (black) are included for reference. *(B)* The mean fluorescence intensity of IFNα in pDCs after imiquimod stimulation is compared between the time point before viremia at which the highest pDC frequency occurred and the time point immediately prior. p-value was calculated with the Wilcoxon test. n = 14 participants from RV397, 11 of whom received VRC01.

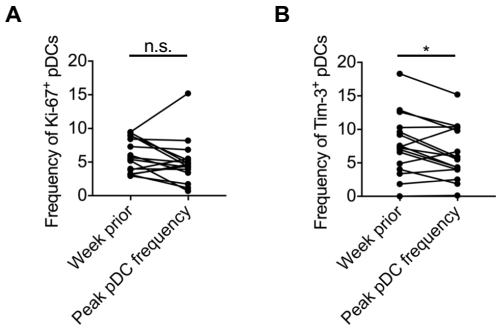

Supplemental Figure 6. Changes in non-functional pDC phenotypes after ATI.

(A) The percentage of pDCs positive for Ki-67 was measured by flow cytometry and compared between the visit with peak pDC frequency and the visit immediately prior. *(B)* The frequency of pDCs expressing Tim-3 was measured by flow cytometry and compared between the week of peak pDC frequency prior to detectable viremia and the week prior (* $p<0.05$, Wilcoxon test).

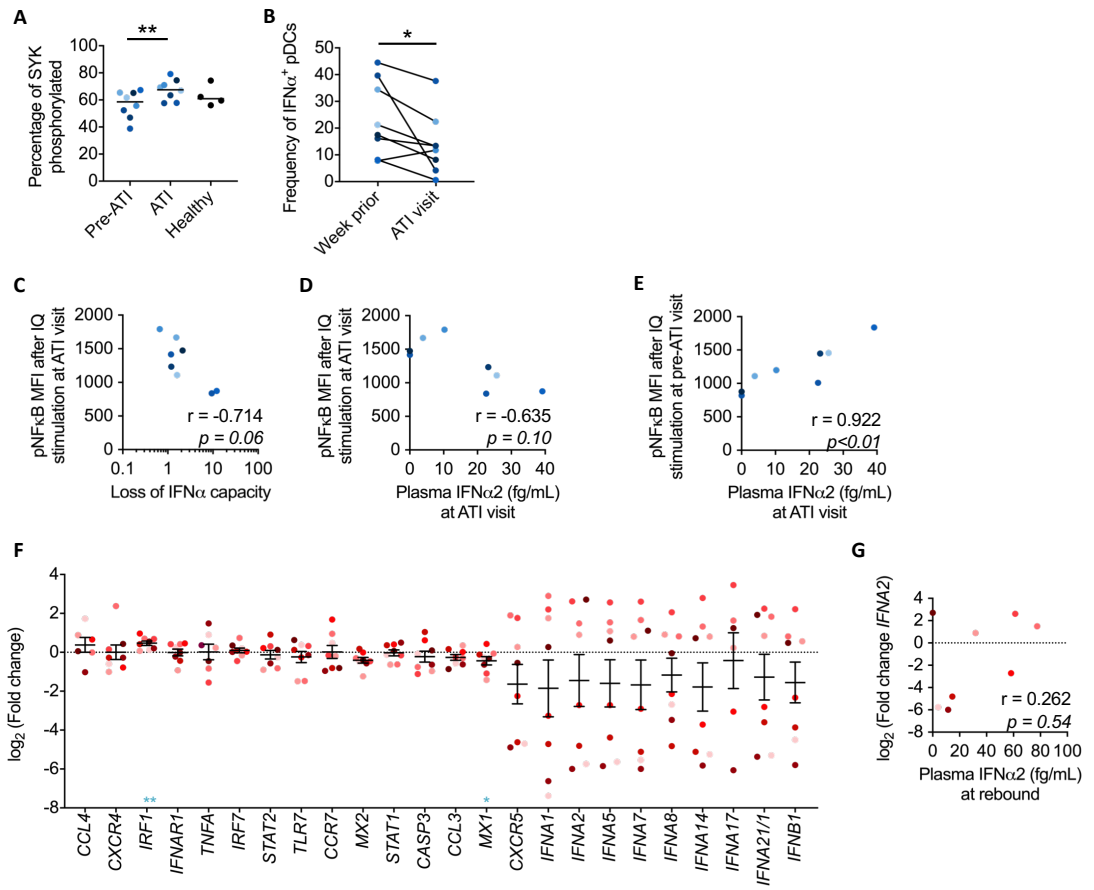

Supplemental Figure 7. Changes in signaling gene expression in mDCs after ATI. *(A)* The basal percentage of SYK that was phosphorylated was measured by flow cytometry immediately after thawing PBMCs from a visit prior to ATI (pre-ATI), after ATI (ATI), and from HIV⁻ healthy Thai individuals (bar represents median percentage, ** $p<0.01$, Wilcoxon test). *(B)* The frequencies of pDCs producing IFNα after imiquimod stimulation are shown for the ATI visit when phosphorylation of IRF7 and NF-κB was measured and the week prior (* $p<0.05$, Wilcoxon test). Loss of IFNα capacity was calculated as the frequency of pDCs producing IFNα at the "Week Prior" visit divided by the ATI visit. *(C)* The phosphorylation levels of NF-κB were measured in pDCs by flow cytometry after in vitro imiquimod stimulation of PBMCs. Spearman correlations were performed between the MFI of NF-κB and the loss in IFNα producing capacity. *(B-C)* Plasma IFNα2 levels were measured by SIMOA. Spearman correlations were performed between the plasma IFNα2 levels at the ATI visit and the MFI of pNF-κB in pDCs from the ATI visit *(B)* or the pre-ATI visit *(C)*. *(F)* Gene expression was measured by BioMark in mDCs sorted from the pre-ATI and ATI visits. Shown is the difference in CT values between the ATI time point and pre-ATI time point after normalization to GAPDH (mean ± SEM, * $p<0.05$, ** $p<0.01$, One sample Wilcoxon test, blue indicates values were no longer significant when corrected for a false discovery rate of 10% by the Benjamin-Hochberg Procedure). *(G)* Spearman correlation between the plasma IFNα2 levels after viral rebound and the change in *IFNA2* levels in mDCs at the ATI time point. *(A-E)* n = 8 participants from RV397, all received VRC01 *(F-G)* n = 8 participants from RV397, 4 of whom received VRC01.

Supplemental Table 1. TaqMan Assay IDs

Gene	TaqMan Assay ID	Gene	TaqMan Assay ID
CASP3	Hs00234387_m1	IFNA7	Hs01652729_s1
CCL3	Hs00234142_m1	IFNA8	Hs00932530_s1
CCL4	Hs99999148_m1	IFNAR1	Hs01066116_m1
CCR7	Hs01013469_m1	IFNB1	Hs01077958_s1
CXCR4	Hs00237052_m1	IRF1	Hs00971965_m1
CXCR5	Hs00540548_s1	IRF7	Hs01014809_g1
GAPDH	Hs99999905_m1	MX1	Hs00895608_m1
IFNA1	Hs00855471_g1	MX2	Hs01550814_m1
IFNA14	Hs00533748_s1	STAT1	Hs01013996_m1
IFNA17	Hs00819693_sH	STAT2	Hs01013123_m1
IFNA2	Hs02621172_s1	TLR7	Hs00152971_m1
IFNA21/1	Hs00353738_s1	TNFA	Hs00174128_m1
IFNA5	Hs00818220_s1		